HOKKAIDO UNIVERSITY

Title	Effect of an ultrathin Fe interlayer on the growth of MnGa and spin-orbit-torque induced magnetization switching
Author(s)	Ogawa, Mineto; Hara, Takuya; Hasebe, Shun et al.
Citation	Applied Physics Express, 16(6), 063002 https://doi.org/10.35848/1882-0786/acdb2c
Issue Date	2023-06-14
Doc URL	https://hdl.handle.net/2115/92652
Rights	© [2023] The Japan Society of Applied Physics
Rights(URL)	https://creativecommons.org/licenses/by-nc-nd/4.0/
Type	journal article
File Information	revised manuscript v2 clean version.pdf



Hokkaido University Collection of Scholarly and Academic Papers : HUSCAP

Effect of an ultrathin Fe interlayer on the growth of MnGa and spin-orbit-torque induced magnetization switching

Mineto Ogawa, Takuya Hara, Shun Hasebe, Michihiko Yamanouchi, and Tetsuya Uemura*

Grad. School of Information Science and Technology, Hokkaido University, Sapporo 060-0814, Japan

E-mail: uemura@ist.hokudai.ac.jp

We investigated the effect of an ultrathin Fe interlayer on the growth of MnGa and spin-orbit torque (SOT) induced magnetization switching. MnGa was epitaxially grown on Fe at room temperature without thermal annealing. The MnGa/Fe bilayer was perpendicularly magnetized, and clear magnetization switching of MnGa/Fe bilayer using the spin current mainly from the adjacent Ta was observed. The insertion of Fe layer reduced the switching current density and increased a SOT-originated effective magnetic field. These results indicate that MnGa/Fe bilayer is a promising spin source, capable of both perpendicular spin injection into GaAs and electrical manipulation of its spin direction.

Electrical injection of polarized spins from ferromagnetic electrodes into semiconductors is a key technology for spin-based semiconductor devices, such as spin transistors, spin light-emitting diodes (spin LEDs), and spin surface-emitting lasers. There have been many reports on spin injection using in-plane magnetized ferromagnets, such as Fe [1,2], CoFe [3,4], and Co_2MnSi [5,6]. Perpendicularly magnetized spin sources are desirable, because ferromagnets with relatively large perpendicular magnetic anisotropy (PMA) can be miniaturized while keeping thermal stability and they are suitable for device integration. Moreover, no magnetic field is needed to inject spins aligned perpendicularly to the plane into semiconductors, which is requisite for application to spin surface-emitting lasers. Spin injection into GaAs has been demonstrated using certain PMA films, such as CoFeB/MgO [7], MnGa [8], and Tb/Fe multilayers [9,10]. Liang *et al* demonstrated perpendicular spin injection into GaAs at room temperature (RT) from CoFeB/MgO injectors by means of spin-LEDs without an external magnetic field [7]. In this system, the MgO layer that was inserted between CoFeB and GaAs induces interfacial PMA [11]. Moreover, the MgO interlayer enhances the spin injection efficiency due to its spin filtering effects [3, 12] and it also suppresses diffusion of atoms between CoFeB and GaAs [13]. On the other hand, the junction resistance increases exponentially with the thickness of MgO [14, 15], which degrades device characteristics, such as the magnetoresistance, transconductance, and current-drive capability. Thus, in the CoFeB/MgO system, obtaining low junction resistance may not be compatible with keeping PMA with sufficient thermal stability.

MnGa is an alternative to the CoFeB/MgO system because it has relatively strong PMA without MgO due to its crystalline magnetic anisotropy, and the PMA has been reported in MnGa thin film with a thickness of a few nm to several tens of nm [8, 16-23]. Moreover it has relatively high spin polarization [24], high Curie temperature [24,25], and small lattice mismatch to GaAs. Adelmann *et al.* reported the spin injection from perpendicularly magnetized δ-MnGa directly grown on GaAs via optical detecting method, but the obtained circular polarization was only a few percent at 2 K [8]. One of the difficulties of spin injection in the MnGa/GaAs system comes from the interfacial reaction between the MnGa and GaAs due to the thermodynamically unstable Mn [26]. Since MnGa directly deposited on GaAs needs a thermal treatment at more than 200 °C in order to be crystallized [17], Mn may diffuse into GaAs, preventing spin injection. Thus, a buffer layer for enabling low-

temperature growth is required. In this study, we focused on inserting an ultrathin Fe layer between the MnGa and GaAs, because spin injection from Fe into GaAs has been clearly demonstrated [1,2]. Moreover, the Fe layer can be perpendicularly magnetized due to the interfacial exchange coupling between MnGa and Fe [18]. Thus, a MnGa/Fe bilayer is expected to be a promising spin source of perpendicular spin injection into GaAs. Accordingly, the first purpose of this study is to clarify the effect of an ultrathin Fe film inserted between MnGa and GaAs on the growth of MnGa and its magnetic properties.

Another issue related to the realization of spin-based semiconductor devices is to develop an electrical manipulation of magnetization direction with high speed, low power, and high write endurance. Conventional magnetic-field switching has difficulty in switching the magnetization of only the selected ferromagnet. Recently, spin-orbit-torque (SOT) induced magnetization switching has attracted attention as a way of selective switching in magnetic random access memory [27,28] and it should be also suitable for the spin-based semiconductor devices. Although SOT-induced magnetization reversal has been reported in perpendicularly magnetized MnGa [19-23], it has not been demonstrated yet in MnGa/Fe bilayer. Thus, the second purpose of this study is to demonstrate SOT-induced magnetization switching in MnGa/Fe bilayer grown on GaAs and clarify the effect of the inserted Fe layer on SOT switching characteristics. For this purpose, we investigated SOT-induced magnetization switching of a MnGa/Fe bilayer with a SOT spin source consisting of Ta.

Layer structures consisting of (from the surface side) Ta (6)/MnGa (2)/Fe (0.6 or 0)/GaAs buffer (250) were deposited on GaAs (001) single-crystal substrate [Fig. 1(a)]. The numbers in parentheses are normal thicknesses in nanometers. The undoped GaAs buffer layer was grown by molecular beam epitaxy (MBE) at 590 ℃ at a growth rate of 1 μm/hour. The sample was capped with an arsenic protective layer and transported in the atmosphere to another chamber. After the arsenic cap was removed by heating the samples to 300 °C, a 0.6-nm-thick Fe film and a 2-nm-thick MnGa were grown at RT by electron beam evaporation and MBE. Finally, Ta was sputtered as the spin source of SOT. The composition of MnGa determined from inductively coupled plasma optical emission spectroscopy measurements was $Mn_{1.8}Ga_1$, suggesting it had a $L1_0$ crystal structure. In order to distinguish the effect of the Fe layer, a sample without a Fe layer was also fabricated, in which the MnGa was directly deposited on the GaAs buffer at RT, and it was annealed at 200-220 ℃ for 15 min. to improve

its crystalline quality.

The crystal structure was confirmed by reflection high energy electron diffraction (RHEED) observations. To evaluate the magnetic properties and SOT-switching characteristics, the structure was processed into Hall devices with a 5-μm-wide channel. The effective magnetic field originating from the SOT was also evaluated by examining the SOT acting on the domain walls (DWs). A schematic of the measurement setup with a definition of the Cartesian coordinate system is shown in Fig. 1(b).

Figure 2 shows RHEED patterns of (a) MnGa/Fe/GaAs and (b) MnGa/GaAs along the [110] azimuth of the GaAs substrate. The GaAs surface showed As-stabilized (2 × 4) patterns just after removing the As cap. The MnGa grown on Fe showed a clear streak pattern, indicating epitaxial growth without thermal annealing. On the other hand, the MnGa directly grown on GaAs showed a halo pattern, indicating an amorphous state, and it was crystallized by annealing at 200-220 ℃ for 15 min, as shown in Fig. 2(b). This result is consistent with the findings of previous studies [17]. Thus, it was confirmed that an ultrathin Fe layer acted as a proper template for the growth of single-crystalline MnGa without a thermal treatment.

We investigated the effect of the inserted Fe layer on the magnetic properties through the anomalous Hall effect (AHE). Figures 3(a) and 3(b) show the transverse resistance R_{yx} measured at RT for MnGa with and without the Fe layer as functions of the out-of-plane magnetic field H_z and in-plane magnetic field H_x along the channel, where μ_0 is the permeability of the vacuum. Since the AHE is dominant in R_{yx} for MnGa [17], R_{yx} reflects the out-of-plane magnetization. Clear square hysteresis was observed in both samples with respect to H_z. The magneto-optical Kerr effect (MOKE) measurement for the MnGa/Fe showed no in-plane component of remanent magnetization (*not shown*). These results indicate that the ultrathin Fe layer was also magnetized perpendicularly due to the interfacial exchange coupling between MnGa and Fe [18]. The magnetic anisotropy field $\mu_0 H_k$ at 290 K for the MnGa/Fe bilayer and the MnGa single layer were estimated to be 2.1 and 3.5 T, respectively, from R_{yx} vs. $\mu_0 H_x$ curves, where the hysteretic behavior observed at low H_x can be caused by unintentional tilt of the device with respect to magnetic field axis. Although the insertion of Fe layer reduced the value of H_k by 40%, the MnGa/Fe bilayer is promising for injection of out-of-plane spins into GaAs because it can be grown on GaAs without annealing.

Now we describe the current-induced magnetization switching for the MnGa(2)/Fe(0.6 or 0) samples. Figure 4 shows the R_{yx} of (a) the MnGa/Fe bilayer and (b) MnGa single layer as a function of pulse current I_P. (see Supplementary-1 for the details of the measurement conditions.) Clear magnetization switching was observed in the MnGa/Fe bilayer. When the directions of I_P and H_x were parallel (antiparallel), the magnetization switched from –z (+z) to +z (–z). This relationship agrees with that expected from the switching of perpendicular magnetization by Slonczewski-like SOT originating from the spin Hall effect (SHE) in the Ta layer [29,30]. The switching current density (J_c) in Ta was 1.5×10^7 A/cm^2, which is comparable to the values reported for SOT switching in Pt/MnGa(2) grown on CoGa-buffered MgO substrate [20]. On the other hand, no clear magnetization switching was observed in the MnGa single layer in the range of ±12 mA. This indicates that the MnGa/Fe bilayer is more suitable for perpendicular spin sources of spin-based semiconductor devices compared with MnGa single layer because the magnetization direction can be switched with a smaller current.

In order to further clarify the effect of the Fe layer on the SOT-induced magnetization switching, we investigated the effective magnetic field H_{eff} originating from SOT. To do this, we measured the current-induced shift in the out-of-plane hysteresis loop under H_x [31]. (see Supplementary-2 for the details of this method.) Figures 5(a) and 5(b) show R_{yx} measured at 250 K as a function of $\mu_0 H_z$ under $\mu_0 H_x$ = 250 mT. A sizable shift of the hysteresis loop was observed depending on the polarity of the current applied to the MnGa/Fe bilayer, while almost no shift was observed for the MnGa single layer. When the applied current and H_x were parallel (antiparallel), the center of the hysteresis loop shifted to the negative (positive) $\mu_0 H_z$ direction for a MnGa/Fe bilayer [Fig. 5(a)]. This indicates that a positive (negative) effective field along z-axis was generated. The direction of the shift is consistent with the polarity of the SOT-induced switching of the MnGa/Fe bilayer with respect to the directions of I_P and H_x shown in Fig. 3(a); that is, when the directions of I_P and H_x were parallel (antiparallel), the magnetization switched from –z (+z) to +z (–z). Thus, this shift can be explained by the generation of H_{eff} originating from the SOT acting on the magnetization in DWs [31], and half of the shift amount corresponds to $\mu_0 H_{eff}$. Figure 5(c) shows $\mu_0 H_{eff}$ as a function of $\mu_0 H_x$ for the MnGa/Fe bilayer and MnGa single layer. The saturation of $\mu_0 H_{eff}$ with respect to $\mu_0 H_x$ was observed for the MnGa/Fe bilayer that was due to realignment of

the internal magnetization in the DWs with H_x, as reported previously [31]. The value of $\mu_0 H_{\mathrm{eff}}$ in the MnGa/Fe bilayer was much larger than that in the MnGa single layer.

According to the macro-spin model, H_{eff} is inversely proportional to the total magnetic moment per area, m_s [32]. Since MnGa and Fe were ferromagnetically coupled [18], m_s was increased by Fe insertion. Nevertheless, a larger H_{eff} was obtained in the MnGa/Fe bilayer. This suggests that the Fe insertion increased the spin current and/or changed the properties of MnGa. In order to clarify the latter effect, however, various further experiments are needed. Here, we discuss the former possibility. Since the RHEED patterns of MnGa for both samples have no significant difference, the quality of Ta deposited on MnGa are almost the same. This suggests that the magnitude of the spin current injected from Ta has no significant difference in both samples. Next we consider the interfaces facing GaAs for both samples. Recently, it was reported that the spin Hall angle was enhanced in $Co_2FeAl_{0.5}Ga_{0.5}$/Ge due to the atomic interdiffusion during annealing [34]. Since MnGa directly deposited on GaAs was also annealed, such interdiffusion may occur. However, no significant enhancement of spin Hall angle was observed in the MnGa/GaAs, which suggests that no interdiffusion occurred or the sign of H_{eff} originating from Ta and that from interdiffusion at the MnGa/GaAs are opposite. On the other hand, in case for the MnGa/Fe bilayer, an effective spin-orbit field (SOF) originating from Rashba and Dresselhaus spin-orbit interactions at Fe/GaAs interface [33] may enhance the SOT efficiency, depending on the sign of SOFs. However, we have no direct evidence for the presence of such SOF in our device (see Supplementary-3). Thus, further systematic studies are needed to clarify the dominant origin.

In summary, we investigated the effect of inserting an ultrathin Fe layer between MnGa and GaAs on the growth of MnGa and SOT-induced magnetization switching. Insertion of Fe enabled epitaxial growth of MnGa at RT with clear PMA including the Fe layer. Moreover, the inserted Fe layer reduced the current density of SOT switching of MnGa. These results indicate that a MnGa/Fe bilayer is a promising out-of-plane spin source of spin-based semiconductor devices capable of magnetization switching with high speed, low power and high reliability.

Acknowledgments

This work was supported in part by the Japan Society for the Promotion of Science KAKENHI (Grant nos. 20H02174 and 20H02598), MEXT X-NICS (JPJ011438), MEXT ARIM (JPMXP1222HK0071), and JST CREST (JPMJCR22C2).

References

1) X. Lou, C. Adelmann, S. A. Crooker, E. S. Garlid, J. Zhang, K. S. M. Reddy, S. D. Flexner, C. J. Palmstrøm, and P. A. Crowell, Nat. Phys. **3**, 197 (2007).
2) G. Salis, A. Fuhrer, R. R. Schlittler, L. Gross, and S. F. Alvarado, Phys. Rev. B **81**, 205323 (2010).
3) X. Jiang, R. Wang, R. M. Shelby, R. M. Macfarlane, S. R. Bank, J. S. Harris, and S. S. P. Parkin, Phys. Rev. Lett. **94**, 056601 (2005).
4) T. Uemura, T. Akiho, M. Harada, K. Matsuda, and M. Yamamoto, Appl. Phys. Lett. **99**, 082108 (2011).
5) T. Akiho, J. Shan, H.-x. Liu, K.-i. Matsuda, M. Yamamoto, and T. Uemura, Phys. Rev. B **87**, 235205 (2013).
6) Y. Ebina, T. Akiho, H.-xi Liu, M. Yamamoto, and T. Uemura, Appl. Phys. Lett. **104**, 172405 (2014).
7) S. H. Liang, T. T. Zhang, P. Barate, J. Frougier, M. Vidal, P. Renucci, B. Xu, H. Jaffrès, J.-M. George, X. Devaux, M. Hehn, X. Marie, S. Mangin, H. X. Yang, A. Hallal, M. Chshiev, T. Amand, H. F. Liu, D. P. Liu, X. F. Han, Z. G. Wang, and Y. Lu, Phys. Rev. B **90**, 085310 (2014).
8) C. Adelmann, J. L. Hilton, B. D. Schultz, S. McKernan, C. J. Palmstrøm, X. Lou, H.-S. Chiang, and P. A. Crowell, Appl. Phys. Lett. **89**, 112511 (2006).
9) N. C. Gerhardt, S. Hövel, C. Brenner, M. R. Hofmann, F.-Y. Lo, D. Reuter, A. D. Wieck, E. Schuster, W. Keune, and K. Westerholt, Appl. Phys. Lett. **87**, 032502 (2005).
10) S. Hövel, N. C. Gerhardt, M. R. Hofmann, F.-Y. Lo, A. Ludwig, D. Reuter, A. D. Wieck, E. Schuster, H. Wende, W. Keune, O. Petracic, and K. Westerholt, Appl. Phys. Lett. **93**, 021117 (2008).
11) S. Ikeda, K. Miura, H. Yamamoto, K. Mizunuma, H. D. Gan, M. Endo, S. Kanai, J. Hayakawa, F. Matsukura and H. Ohno, Nat. Mater. **9,** 721 (2010).
12) W. H. Butler, X.-G. Zhang, T. C. Schulthess, and J. M. MacLaren, Phys. Rev. B **63**, 054416 (2001).
13) G. Hoffmann, B. Jenichen, and J. Herfort, J. Cryst. Growth, **512**, 194 (2019).
14) T. Akiho, T. Uemura, M. Harada, K.-i. Matsuda, and M. Yamamoto, Appl. Phys. Lett. **98**, 232109 (2011).
15) G. Hoffmann, J. Herfort, and M. Ramsteiner, Phys. Rev. Materials **3**, 074402 (2019).
16) L. J. Zhu, D. Pan, S. H. Nie, J. Lu, and J. H. Zhao, Appl. Phys. Lett. **102**, 132403 (2013).
17) M. Tanaka, J. P. Harbison, J. DeBoeck, T. Sands, B. Philips, T. L. Cheeks, and V. G. Keramidas, Appl. Phys. Lett. **62**, 1565 (1993).
18) Q. L. Ma, S. Mizukami, T. Kubota, X. M. Zhang, Y. Ando, and T. Miyazaki, Phys. Rev. Lett. **112**, 157202 (2014).
19) K. Meng, J. Miao, X. Xu, Y. Wu, J. Xiao, J. Zhao and Y. Jiang, Sci Rep **6**, 38375 (2016).

20) M. Takikawa, K. Z. Suzuki, R. Ranjbar, and S. Mizukami, Appl. Phys. Express **10** 073004 (2017).
21) R. Ranjbar, K. Z. Suzuki, S. Mizukami, J. Magn. Magn. Mater. **456**, 22 (2018).
22) M. Yamanouchi, N. V. Bao, F. Shimohashi, K. Jono, M. Inoue, and T. Uemura, AIP Advances **9**, 125245 (2019).
23) K. Jono, F. Shimohashi, M. Yamanouchi, and T. Uemura, AIP Advances **11**, 025205 (2021).
24) B. Balke, G. H. Fecher, J. Winterlik, and C. Felser, Appl. Phys. Lett. **90**, 152504 (2007).
25) J. Kübler, J. Phys.: Condens. Matter **18**, 9795 (2006).
26) J. L. Hilton, B. D. Schultz, S. McKernan, and C. J. Palmstrøm, Appl. Phys. Lett. **84**, 3145 (2004).
27) I. M. Miron, K. Garello, G. Gaudin, P.-J Zermatten, M. V. Costache, S. Auffret, S. Bandiera, B. Rodmacq, A. Schuhl and P. Gambardella, Nat. **476**, 189 (2011).
28) S. Fukami, and H. Ohno, Jpn. J. Appl. Phys. **56** 0802A1 (2017).
29) L. Liu, C. Pai, Y. Li, H. W. Tseng, D. C. Ralph, and R. A. Buhrman, Science **336**, 555 (2012).
30) M. Cubukcu, O. Boulle, M. Drouard, K. Garello, C. O. Avci, I. M. Miron, J. Langer, B. Ocker, P. Gambardella, and G. Gaudin, Appl. Phys. Lett. **104**, 042406 (2014).
31) C.-F. Pai, M. Mann, A. J. Tan, and G. S. D. Beach, Phys. Rev. B **93**, 144409 (2016).
32) A. Thiaville, S. Rohart, É. Jué, V. Cros, and A. Fert, EPL Europhys. Lett., **100**, 57002 (2012).
33) L. Chen, M. Decker, M. Kronseder, R. Islinger, M. Gmitra, D. Schuh, D. Bougeard, J. Fabian, D. Weiss, and C.H. Back, nat. commun. **7**, 13802 (2016).
34) S. Kaneta-Tanaka, M. Yamada, S. Sato, S. Arai, L. Anh. K. Hamaya, and S. Ohya, Phys. Rev. Appl. 14. 024096 (2020).

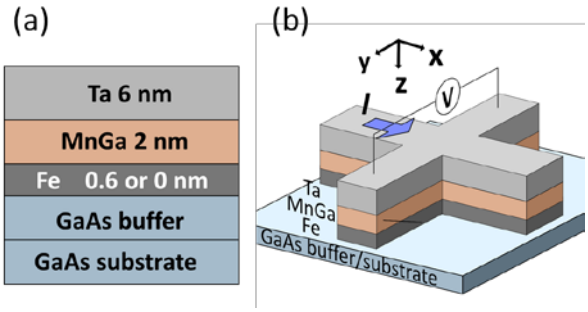


Fig. 1. Schematic of (a) layer structure and (b) a Hall bar device with a 5-μm wide channel and a pair of Hall probes, together with a definition of the Cartesian coordinate system. Transverse resistance R_{yx} was measured with an in-plane dc current I under application of external magnetic fields: in-plane magnetic field (H_x) and out-of-plane magnetic field (H_z).

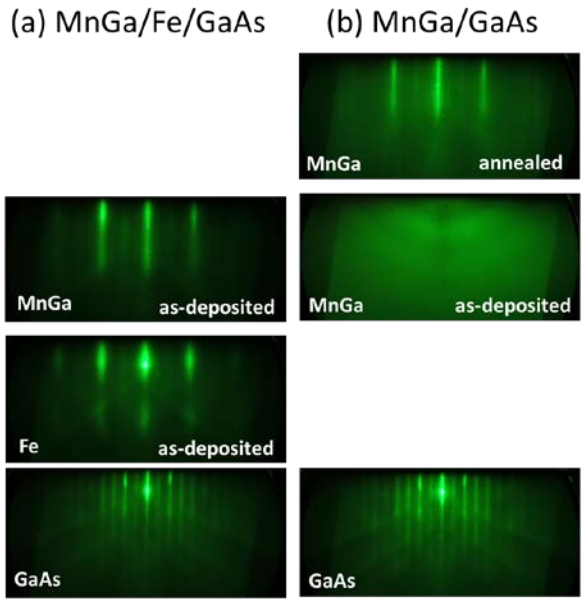


Fig. 2. RHEED patterns of (a) MnGa/Fe/GaAs and (b) MnGa/GaAs. The electron beam is incident along the [110] azimuth of GaAs substrate.

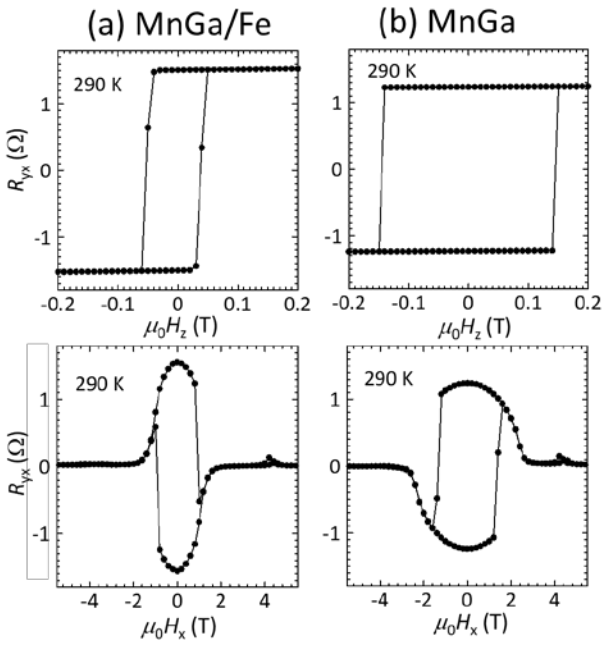


Fig. 3. Transverse resistance R_{yx} measured at 290 K for (a) MnGa/Fe bilayer and (b) MnGa single layer as functions of in-plane and out-of-plane magnetic field.

.

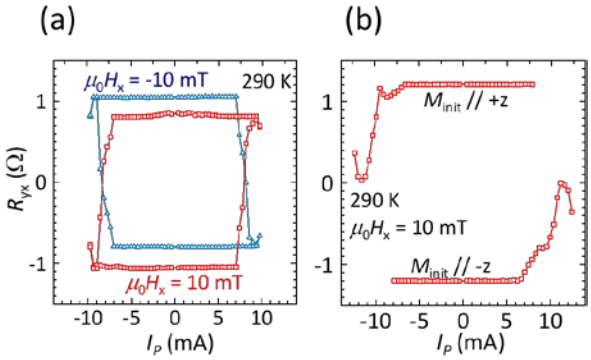


Fig. 4. Transverse resistance R_{yx} measured at 290 K for (a) MnGa/Fe bilayer and (b) MnGa single layer as a function of pulse current.

.

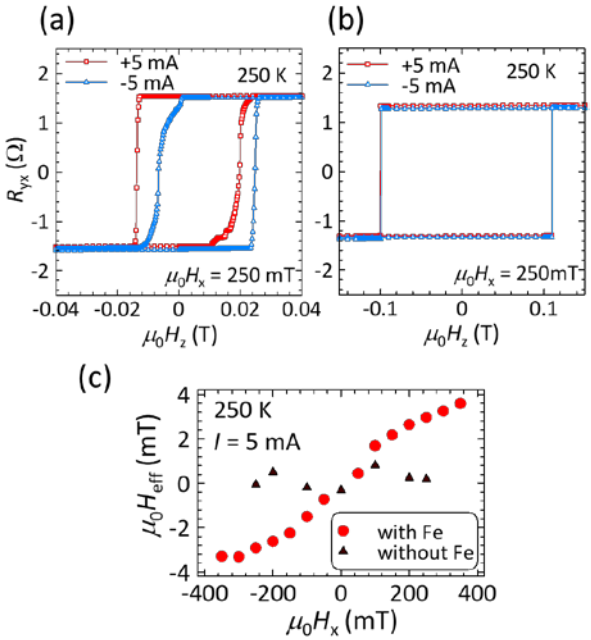


Fig. 5. Transverse resistance R_{yx} measured at 250 K as a function of $\mu_0 H_z$ with a dc current I = ±5 mA under $\mu_0 H_x$ = +250 mT for (a) MnGa/Fe bilayer and (b) MnGa single layer. (c) $\mu_0 H_{\text{eff}}$ at I = 5 mA as a function of $\mu_0 H_x$ for a MnGa/Fe bilayer and a MnGa single layer.